

CONFINING PRESSURE EFFECT ON THE PERMEABILITY AND MECHANICAL BEHAVIOR OF SANDSTONE UNDER A CERTAIN PORE WATER PRESSURE CONDITION

by

**Wei-Qiang LING^{a,c}, He-Ping XIE^{a,b}, Yi-Hang LI^{d,e},
Ze-Tian ZHANG^{d,e}, and Li REN^{b,c*}**

^aShenzhen Key Laboratory of Deep Underground Engineering Sciences and Green Energy,
Shenzhen University, Shenzhen, Guangdong, China

^bMOE Key Laboratory of Deep Earth Science and Engineering, Sichuan University, Chengdu, China

^cCollege of Architecture and Environment, Sichuan University, Chengdu, China

^dCollege of Water Resource and Hydropower, Sichuan University, Chengdu, China

^eState Key Laboratory of Hydraulics and Mountain River Engineering,
Sichuan University, Chengdu, China

Original scientific paper

<https://doi.org/10.2298/TSCI2301647L>

In geotechnical engineering, the mechanical behavior of rocks under various In-situ conditions (stress state including axial stress, confining pressure, pore water pressure) have always been an important topic. Therefore, the confining pressure effect on the permeability and mechanical behavior of different size sandstone samples under a certain pore water pressure condition was studied. The permeability of different sizes samples shows roughly the same exponential decreasing law with the increase of confining pressure. In the mechanical behavior test, both the loading Young's modulus E^+ and the unloading Young's modulus E^- increased continuously with increasing confining pressure, while the unloading Poisson's ratio μ^- decreased to a certain value and then remained almost constant.

Key words: confining pressure effect, permeability, mechanical behavior, sandstone, porous

Introduction

When underground engineering enters deeper horizons, the insitu geo-environment becomes critically complex. The geo-stresses and pore pressure are increasingly prominent with burial depth [1-3]. To ensure the stability and safety of deep underground engineering, the mechanical behavior of rocks under various in situ conditions has become an important research topic in the field of rock mechanics.

In fact, the internal structure of rock materials (pores, cracks, foliation) undergoes complex changes (dense, broken, self-locking, etc.) under various in situ conditions, resulting in changes in the parameters characterizing the basic physical and mechanical properties of materials, such as Young's modulus, Poisson's ratio, strength, and permeability. This eventually caused a special deep mechanical behavior different from the norm. To date, many stud-

*Corresponding author, e-mail: renli-scu@hotmail.com

ies have investigated the permeability and mechanical behavior of rocks under various in situ conditions, which helped to establish a constitutive model of rocks applicable to the real deep environment. Zhu *et al.* [4] conducted triaxial compression experiments to investigate the influences of stress and failure mode on the axial permeability of five sandstones with porosities ranging from 15% to 35%. Jiang *et al.* [5] examined the deformation and failure characteristics of granite at different depths by triaxial tests at various pressures and temperatures. Zhou *et al.* [6] found that the Young's modulus increases linearly with the increase of rock depth, while Poisson's ratio decreases. Li *et al.* [7] proposed a new pressure-permeability relationship based on a new void ratio-pressure model and Kozeny-Carman equation. Xie *et al.* [8] conducted laboratory tests and mining mechanics simulations on coal samples recovered from 1000 m or deeper and found that the tensile strength and deformation of the deep coal rocks were generally small when destroyed. However, there are few studies that consider the effect of the confining pressure on the permeability evolution. The pore water pressure is not considered in the traditional study of the confining pressure effect on the mechanical behavior of rocks. Studies on the simultaneous evolution of permeability and elastic parameters of rocks with various stress states under the same pore water pressure conditions are rare.

In this work, a series of experiments were carried out on sandstone samples to test the permeability and mechanical behavior under a certain pore water pressure and different confining pressure conditions. The effect of the dimension on the permeability under different confining pressures was preliminarily investigated. The stress-strain behavior of sandstone during loading and unloading with different confining pressures under 6 MPa pore water pressure was explored.

Experimental methods

Samples

The standard sandstone samples, fig. 1(a), were prepared with dimensions of diameter, D 50 mm \times height, H 100 mm as recommended by the International Society of Rock Mechanics (ISRM). In addition, a small sandstone sample was prepared with dimensions of D 50 mm \times H 40 mm. The Nuclear Magnetic Resonance Core Analysis System was used to test the initial porosity of several sandstone samples after fully saturated treatment and to simply extrapolate the permeability.

Experimental procedure

The experiments in this paper were carried out using the MTS815 Flex Test GT Rock Mechanics Test System, fig. 1(b). The confining pressure effect experiments included two parts: a permeability test and a mechanical behavior test. The pore water pressure was 6 MPa.

In the permeability test, the test procedure was as follows: First, the sample (#1, #s1) was installed into the triaxial pressure chamber, and the installation of the annular and axial sensors and their seepage channels was checked. Second, a hydrostatic pressure state (10 MPa) was applied. Third, the initial pressure differential, ΔP_i , was set to approximately 6 MPa. The seepage upstream and downstream water pressure pumps and their valves were closed to form a confined space inside. Fourth, after waiting for a period, Δt , record the final pressure differential, ΔP_f . Afterwards, the hydrostatic pressure was increased to 20 MPa, 40

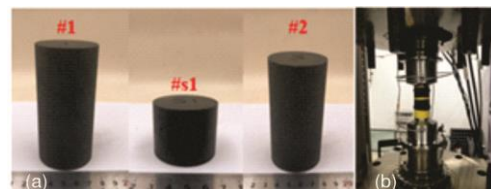


Figure 1. Samples and apparatus; (a) samples and (b) testing apparatus

MPa, 60 MPa, 80 MPa, and 100 MPa according to the same previous procedure, and the transient permeability testing method was carried out.

The permeability k_p is calculated by the transient permeability equation using the water decay law, *i.e.*:

$$k_p = \mu_0 \beta_0 V \left[\frac{\ln \left(\frac{\Delta P_i}{\Delta P_f} \right)}{2 \Delta t \left(\frac{A_s}{L_s} \right)} \right] \quad (1)$$

where V is the reference volume, L_s – the length of the sample, A_s – the cross-sectional area of the sample, μ_0 [Pa s] – the viscosity of the pore fluid, and β_0 – the compressibility of the pore fluid. All the parameters are constants in this test.

In the mechanical behavior test, the pore water pressure was set to 6 MPa. The confining pressures were 10 MPa, 20 MPa, 40 MPa, and 80 MPa. The loading and unloading paths were depicted in fig. 2. The test procedure was as follows: First, sample #2 was installed into the triaxial pressure chamber, and the installation of the annular and axial sensors and their seepage channels was checked. Second, a hydrostatic pressure state of $\sigma_1 = \sigma_2$

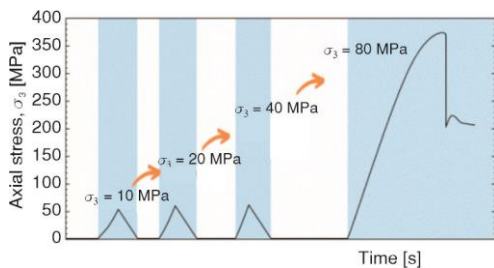


Figure 2. Stress paths for confining pressure loading and axial stress loading and unloading in the mechanical behavior test

(σ_3) = 10 MPa was applied to sample #2. Third, the pore water pressure was loaded and remained at 6 MPa. Fourth, the axial pressure was loaded and unloaded. Afterwards, the hydrostatic pressure was increased to 20 MPa, 40 MPa, and 80 MPa according to the same procedure, and the deformation of the sample in different directions was recorded. Finally, sample #2 was monotonically loaded until failed under a confining pressure of 80 MPa.

Results and analysis

Permeability characteristics

From fig. 3, the permeability of different size samples decreased exponentially with increasing confining pressure. The permeability of rock is a combined measure of porosity, pore size and pore tortuosity, which are closely related to the external stress environment. As the confining pressure increased, the circumferential constraint of the rock sample itself increased, the native fractures (pores) inside the rock sample were suppressed and compacted, and the permeability throat became narrower and less, which led to a gradual decrease in permeability. The correlation between the permeability and porosity of porous media can most commonly be described by the Kozeny-Carman model [9-11] in the following form:

$$k_p = \frac{\phi^3}{c \tau^2 S^2} \quad (2)$$

where ϕ is the porosity, S – the surface area per unit volume, τ – the tortuosity of the medium, and c – the Kozeny constant that depends on the geometry of the porous sample.

The effect of sample dimension on the permeability was concerned. It is found that the permeability of the small sample (#s1) was slightly larger than that of the standard sample (#1) under the same confining pressure. However, the Nuclear Magnetic Resonance results

showed that the porosity and permeability of the small sample were instead smaller than those of the standard sample in the initial no-confining pressure condition: the standard sample (#1), 6.1% and $4.35 \cdot 10^{-17} \text{ m}^2$, the small sample (#s1), 5.8% and $3.38 \cdot 10^{-17} \text{ m}^2$. The effect of the confining pressure reversed the comparative relationship between the permeability of the standard sample and that of the small sample. In addition, the difference between the permeability of the two samples (Δk_p) decreased with the confining pressure loading. The permeability of different size samples tends to be the same under the high confining pressure condition $\sigma_3 \geq 60 \text{ MPa}$.

The permeability variation laws of samples of different sizes under different confining pressures obtained from the tests were fitted using the models proposed by Gangi [12], Walsh [13], Chen [14], and Li [7]. The predicted values of permeability and their relative errors are listed in tabs. 1 and 2. The comparisons between the measured data and the fitted curves are shown in fig. 4. A simple index was used to evaluate the applicability of the permeability evolution model. The comparison of the fitted results revealed that the model of Gangior Walsh was more suitable for describing the permeability evolution of sandstone with confining pressure loading under this condition. The best-fit equations were similar for different sizes of sandstone samples. However, the permeability evolution law of the small sandstone sample is slightly worse than that of the standard sandstone sample.

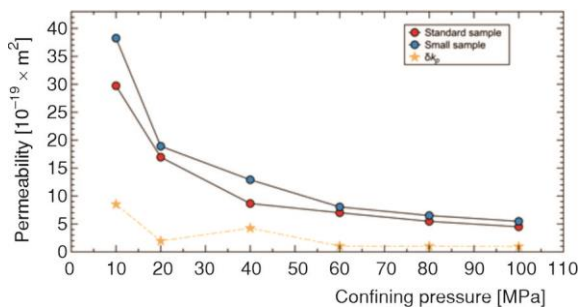


Figure 3. Permeability variations under various confining pressures for different size samples

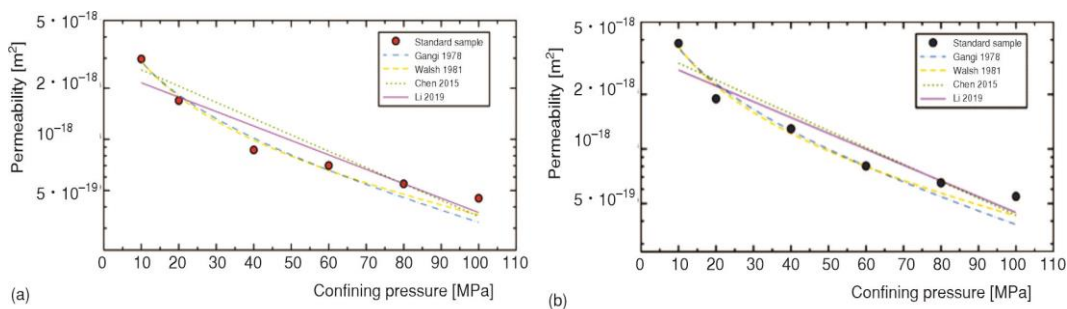


Figure 4. Comparisons between the measured data and the fitted curves for samples under different confining pressures; (a) Sample #1 and (b) Sample #s1

Mechanical behavior

The stress-strain behavior and basic mechanical properties of the sandstone sample under different confining pressure conditions were investigated. As shown in fig. 5, the rock retained a certain non-recoverable strain after unloading under different confining pressures. Even though the reference point axial stress is much lower than the yield stress and the peak stress, the unloading curve and the loading curve could still not coincide and deviate far from each other. The loading and unloading curves formed an *ox horn*-like curve. The hysteresis loop of the strain-strain curve with a multistyled shape was created. This is due to the difficulty of closing the pores inside the sandstone under this condition compared to the case of no pore water pressure. Sandstone is a multiphase, multicomponent, non-homogeneous natural

Table 1. Permeability of sandstone for Sample #1 under different confining pressures

Confining pressure σ_3 [MPa]	Experimental permeability ($\times 10^{-19} \text{ m}^2$)	Fitted permeability and percent relative errors			
		$k_p = k_{p0} [1 - (p/c_2)^{c_1}]^3$ [12]	$k_p = k_{p0} [1 - c_1 \ln(p/c_2)]^3$ [13]	$k_p = k_{p0} \exp[c_1(p - c_2)]$ [14]	$k_p = c_3 \left[\frac{\exp(-c_2 p)^3}{1 + c_1 \exp(-c_2 p)} \right]$ [7]
10	29.73	28.65 (4%)	29.08 (2%)	25.65 (14%)	21.53 (28%)
20	16.95	18.26 (8%)	17.78 (5%)	20.57 (21%)	17.70 (4%)
40	8.66	10.17 (17%)	9.87 (14%)	13.23 (53%)	11.97 (38%)
60	7.01	6.57 (6%)	6.58 (6%)	8.51 (21%)	8.10 (16%)
80	5.47	4.54 (17%)	4.75 (13%)	5.47 (0%)	5.48 (0%)
100	4.50	3.25 (28%)	3.59 (20%)	3.52 (22%)	3.70 (18%)
Correlation coefficient		0.983	0.991	0.886	0.896
Applicability		***	****	*	**

geological material formed by the cementation of many minerals. Under the long-term sedimentary environment, many cracks, joints, pores, and other micro-structures are distributed between mineral particles. Furthermore, the pore water pressure of 6 MPa supported the internal pores of sandstone, which makes the non-linear characteristics of sandstone samples more prominent under this working condition. With the loading of axial stress, the internal pores of the sample gradually closed, the stress-strain curve was upwardly convex, the deformation behavior showed *strain hardening*, and the overall stiffness of the material increased. The same is true for the stress-strain behavior during unloading. In fact, at low confining pressure ($\sigma_3 = 10 \text{ MPa}$), the significant non-linearity was characteristic of the stress-strain behavior during loading and unloading. With increasing confining pressure, this non-linear characteristic gradually weakened. In other words, it is almost impossible for us to obtain accurate rock elastic parameters, which will bring root unknowns to deep engineering stability prediction. The elastic parameters, such as E^+ , E^- , μ^+ or μ^- obtained in this paper also only represent the apparent parameters of a certain loading and unloading stage but were not real.

Table 2. Permeability of sandstone for Sample #s1 under different confining pressures

Confining pressure σ_3 (MPa)	Experimental permeability ($\times 10^{-19} \text{ m}^2$)	Fitted permeability and percent relative errors			
		$k_p = k_{p0} [1 - (p/c_2)^{c_1}]^3$ [12]	$k_p = k_{p0} [1 - c_1 \ln(p/c_2)]^3$ [13]	$k_p = k_{p0} \exp[c_1(p - c_2)]$ [14]	$k_p = c_3 \left[\frac{\exp(-c_2 p)^3}{1 + c_1 \exp(-c_2 p)} \right]$ [7]
10	38.25	36.06 (6%)	36.75 (4%)	29.70 (22%)	27.21 (29%)
20	18.91	22.93 (21%)	22.24 (18%)	23.97 (27%)	22.26 (18%)
40	12.91	12.63 (2%)	12.17 (6%)	15.62 (21%)	14.89 (15%)
60	8.05	8.04 (0%)	8.00 (1%)	10.18 (26%)	9.96 (24%)
80	6.51	5.46 (16%)	5.71 (12%)	6.63 (2%)	6.67 (2%)
100	5.47	3.83 (30%)	4.27 (22%)	4.32 (21%)	4.46 (18%)
Correlation coefficient		0.968	0.979	0.901	0.907
Applicability		***	****	*	**

Young's modulus and Poisson's ratio are common elastic parameters used to characterize the deformability of a material in a certain state. Qualitative understanding of the trends of Young's modulus and Poisson's ratio of sandstone with the confining pressure under a certain pore water pressure is meaningful for the construction of the ontological model of sandstone at different depths under the seepage field. Figure 6 depicts the variation trends of elas-

tic parameters with the confining pressure. With increasing confining pressure, both the loading Young's modulus, E^+ , and the unloading Young's modulus, E^- , increased continuously. The unloading Poisson's ratio, μ^- , decreased to a certain value and then remained almost constant. However, the variation pattern of loading Poisson's ratio, μ^+ , was not obvious.

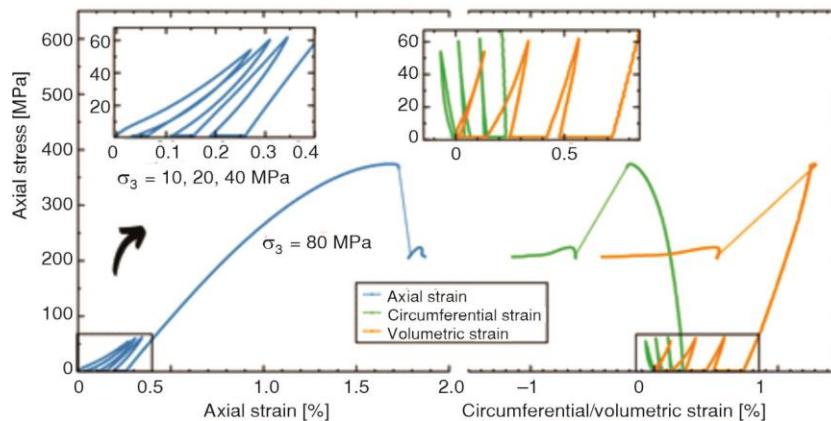


Figure 5. Complete stress-strain curve of the sandstone sample

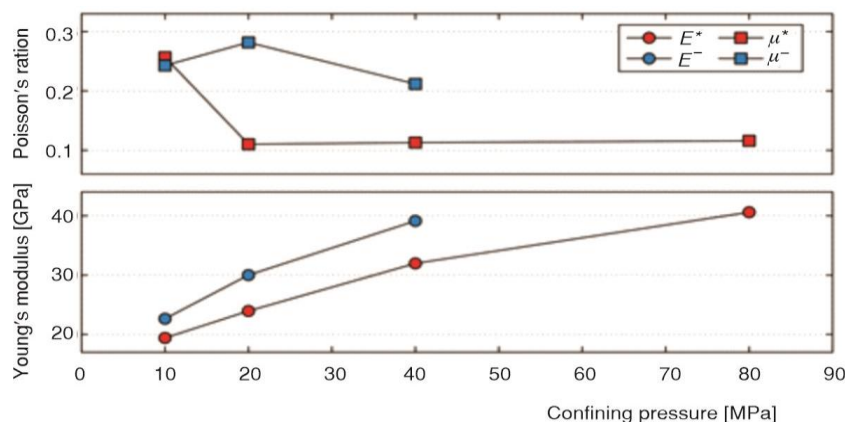


Figure 6. The elastic parameters of the sandstone sample

Understanding the degree of confining pressure effect on the elastic parameters of rocks under the same pore water pressure environment is of great value for permeability prediction and seepage simulation under engineering in-situ conditions [15]. On the one hand, the confining pressure effect made the physical properties of the medium itself change [16], which in turn affected the evolution of permeability with the change in confining pressure. On the other hand, the elasticity parameters reflected the macroscopic deformation capacity of rocks, which could also reflect the magnitude of the permeability to a certain extent. Therefore, it seems feasible to relate elastic parameters to permeability through porosity.

Conclusion

The permeability and mechanical behavior under a certain pore water pressure and different confining pressure conditions were studied. The permeability of different size samples

decreased exponentially with increasing confining pressure. However, the permeability of the small sample was slightly larger than that of the standard sample under a low confining pressure (10 MPa, 20 MPa, and 40 MPa) but tended to be the same under a high confining pressure (60 MPa, 80 MPa, and 100 MPa). In the environment of a certain pore water pressure and a low confining pressure (10 MPa), the sandstone has significant nonlinear stress-strain behavior in the initial compaction stage. With increasing confining pressure, both the loading Young's modulus, E^+ , and the unloading Young's modulus, E^- , increased continuously, while the unloading Poisson's ratio, μ^- , decreased to a certain value and then remained almost constant.

Acknowledgment

The study was financially supported by the National Natural Science Foundation of China (Grant No.51827901).

Nomenclature

A_s	– cross sectional area of sample, [cm ²]	V	– Reference volume, [cm ³]
c	– Kozeny constant, [–]	<i>Greek symbols</i>	
E^+	– loading Young's modulus, [GPa]	β_0	– compressibility of pore fluid, [Pa ⁻¹]
E^-	– unloading Young's modulus, [GPa]	μ^+	– loading Poisson's ratio, [–]
k_p	– permeability, [m ²]	μ^-	– unloading Poisson's ratio, [–]
k_{p0}	– zero pressure permeability, [m ²]	μ_0	– viscosity of pore fluid, [Pa s]
ΔP_i	– initial pressure differential, [MPa]	τ	– tortuosity of the medium, [–]
ΔP_f	– final pressure differential, [MPa]	ϕ	– porosity, [%]
p	– effective pressure, [MPa]		
S	– Surface area per unit volume, [m ⁻¹]		

References

- [1] Zhou, H. W., et al., Developments in Researches on Mechanical Behaviors of Rocks Under the Condition of High Ground Pressure in the Depths, *Advances in mechanics*, 35 (2005), 1, pp. 91-99
- [2] Xie, H. P., Research Framework and Anticipated Results of Deep Rock Mechanics and Mining Theory, *Advanced Engineering Sciences*, 49 (2017), 2, pp. 1-16
- [3] Xie, H. P., et al., Theoretical and Technological Exploration of Deep in Situ Fluidized Coal Mining, *Frontiers in Energy*, 13 (2019), 4, pp. 603-611
- [4] Zhu, W. L., Wong, T. F., The Transition from Brittle Faulting to Cataclastic Flow: Permeability Evolution, *Journal of Geophysical Research: Solid Earth*, 102 (1997), B2, pp. 3027-3041
- [5] Jiang, H. K., et al., Granite Deformation and Behavior of Acoustic Emission Sequence Under the Temperature and Pressure Condition at Different Crust Depths, *Acta Seismologica Sinica*, 13 (2000), 4, pp. 424-433
- [6] Zhou, H. W., et al., Experimental Study of the Effect of Depth on Mechanical Parameters of Rock, *Chinese Science Bulletin*, 55 (2010), 34, pp. 3276-3284
- [7] Li, C. G., et al., Permeability of Porous Media Under Confining Pressure, *Geophysical Journal International*, 216 (2019), 3, pp. 2017-2024
- [8] Xie, H. P., et al., Study on the Mechanical Properties and Mechanical Response of Coal Mining at 1000 m or Deeper, *Rock Mechanics and Rock Engineering*, 52 (2019), 5, pp. 1475-1490
- [9] Kozeny, J., Uber Kapillare Leitung Der Wasser in Boden, *Royal Academy of Science, Vienna, Proc. Class I*, 136 (1927), 1, pp. 271-306
- [10] Carman, P.C., Fluid Flow Through Granular Beds, *Chemical Engineering Research and Design*, 75 (1997), Suppl., pp. S32-S48
- [11] Carman, P. C., *Flow of Gases Through Porous Media*, Academic Press, New York, USA, 1956
- [12] Gangi, A. F., Variation of Whole and Fractured Porous Rock Permeability with Confining Pressure, *International Journal of Rock Mechanics and Mining Sciences*, 15 (1978), 5, pp. 249-257
- [13] Walsh, J. B., Effect of Pore Pressure and Confining Pressure on Fracture Permeability, *International Journal of Rock Mechanics and Mining Sciences*, 18 (1981), 5, pp. 429-435

- [14] Chen, D., *et al.*, Dependence of Gas Shale Fracture Permeability on Effective Stress and Reservoir Pressure: Model Match and Insights, *Fuel*, 139 (2015), pp.383-392
- [15] Dong, J. J., *et al.*, Stress-Dependence of the Permeability and Porosity of Sandstone and Shale from TCDP Hole-A, *International Journal of Rock Mechanics and Mining Sciences*, 47 (2010), 7, pp. 1141-1157
- [16] Ai T., *et al.*, Changes in the Structure and Mechanical Properties of a Typical Coal Induced by Water Immersion, *International Journal of Rock Mechanics and Mining Sciences*, 138 (2021), 7, pp.104597